

Scission neutrons for U, Pu, Cm, and Cf isotopes: Relative multiplicities calculated in the sudden limit

R. Capote,¹ N. Carjan,^{2,3,4} and S. Chiba²

¹*NAPC–Nuclear Data Section, International Atomic Energy Agency, 1400 Vienna, Austria*

²*Research Laboratory for Nuclear Reactors, Tokyo Institute of Technology, 8550 Tokyo, Japan*

³*Joint Institute for Nuclear Research, 141980 Dubna, Moscow Region, Russia*

⁴*Centre d'Etudes Nucleaires de Bordeaux-Gradignan, UMR 5797, CNRS/IN2P3–University Bordeaux I, BP 120, 33175 Gradignan Cedex, France*

(Received 15 October 2015; published 16 February 2016)

The multiplicities of scission neutrons ν_{sc} are calculated for series of U, Pu, Cm, and Cf isotopes assuming a sudden transition between two different nuclear configurations ($\alpha_i \rightarrow \alpha_f$): one just before the neck rupture and one immediately after the disappearance of the neck. This calculation requires only the knowledge of the corresponding two sets of neutron eigenstates. The nuclear shapes around the scission point are described in terms of Cassinian ovals with only two parameters: α (that positions the shape with respect to the zero-neck shape) and α_1 (that defines the mass asymmetry). Based on these shapes, a neutron mean field of the Woods-Saxon type is constructed using two prescriptions to calculate the distance to the nuclear surface. The accent in the present work is put on the dependence of ν_{sc} on the neutron number N_f of the fissioning nucleus and on the mass asymmetry A_L/A_H of the primary fission fragments. The relative dependence of these multiplicities, averaged over the mass yields, $\langle \nu_{sc} \rangle$, are finally compared with existing experimental data on prompt fission neutrons $\langle \nu_p \rangle$.

DOI: [10.1103/PhysRevC.93.024609](https://doi.org/10.1103/PhysRevC.93.024609)

I. INTRODUCTION

The strong and rapid variation of the potential energy in the region between the nascent fission fragments during the scission process (neck rupture) was invoked, in the sixties, as a possible cause for the emission of scission neutrons (SN) [1] and light charged particles [2]. More recently, this idea was developed quantitatively in a quantum-mechanical microscopic frame. Two types of approaches have been proposed: one stationary [3–5] and one time dependent [6,7].

The stationary approach is based on the sudden approximation that consists in assuming that scission occurs at finite neck radius r_{\min} and that the neck stubs are suddenly absorbed by the fission fragments. The neutrons present in the fissioning nucleus before scission (deformation α_i) will suddenly find themselves in a postscission potential (deformation α_f). Consequently they will be described by wave packets with some components in the continuum. The only thing we need to know are the two sets of neutron eigenstates at the two deformations involved.

In reality the scission time ΔT is short but not zero. This means that the neutron wave functions are no more the same at α_f as they were at α_i but have evolved instead. To simulate their evolution one has to solve, for each neutron state, the two-dimensional time-dependent Schrödinger equation (TDSE2D) with a time-dependent potential (TDP). This is clearly a more time-consuming endeavor.

In both models, all neutrons of the fissioning nucleus are partially released during the neck rupture (each with quite small probability). They leave the system immediately thereafter, i.e., during the acceleration of the fission fragments. The sum of these probabilities (properly weighted) gives the number of neutrons per fission event that are left unbound at the end of the scission process. This is what we call

scission-neutron multiplicities ν_{sc} in the present study. These values represent only upper limits for the following reason: due to the partial reabsorption of the neutrons by the fragments not all initially unbound states lead to unbound asymptotic states; the imaginary potential removes neutron flux from the elastic channel. When the sudden approximation is used, there is an extra reason: ν_{sc} is the largest for $\Delta T = 0$ and increasing ΔT decreases ν_{sc} [6].

Very recently the dynamical scission model [6] was applied to the calculation of the angular distribution (with respect to the fission axis) of the average energy distribution (in the laboratory system) as well as of the multiplicity of the scission neutrons emitted from ^{236}U [8]. The surprising result was that, contrary to the general belief, SN have similar properties with the prompt fission neutrons (PFN) measured in the reaction ($n_{th} + ^{235}\text{U}$).

At this point it is appropriate to mention that the hypothesis that all PFN are evaporated from fully accelerated fragments was quite successful. This hypothesis goes back to the early days of fission studies as discussed in Refs. [9,10] and it is the “Los Alamos” model [12] that has been employed in all PFN evaluations for applied purposes. Recently refined, by including the fission fragment deexcitation in the frame of a Monte Carlo type of approach [13–15], the “evaporation” hypothesis can account, with adjusted parameters, for a large amount of experimental data. For instance 95% of the PFN spectrum can be reproduced [16]. So far, the small percentage of PFN that cannot be reproduced by the evaporation hypothesis are considered to be SN (e.g., see Refs. [16–19] and references therein).

New applications of the above mentioned scission models to other observables and other fissioning systems are desirable. The goal of the present paper is to estimate the SN multiplicities for series of U, Pu, Cm, and Cf isotopes and to study in

this way their dependence on the neutron number N_f of the fissioning nucleus. Due to the large number of nuclei involved this can be achieved only in the “sudden” limit; it is the only tractable approach for a systematic study.

As compared with previous publications [3–5] a different extremely deformed nuclear potential, a different method to solve the eigenvalue problem, and a more precise way to calculate the overlap integrals are used.

The eigenvalue problem for a neutron in the deformed mean field of its interaction with the other nucleons is solved in a cylindrical (ρ, z) -coordinate system by diagonalizing the corresponding Hamiltonian in a deformed oscillator basis (as in the Nilsson model [20] or in the deformed Woods-Saxon generalizations that followed [21–24]). More details are given in Sec. II. The two nuclear configurations that define the scission process are discussed in Section III. The formulas used to calculate the scission neutron multiplicities are described in Sec. IV. The neutron multiplicities calculated as a function of the mass asymmetry (defined by the light fragment mass A_L) are presented in Sec. V for all studied fissioning nuclei. The values averaged over the mass yields are compared, in Sec. VI, with the existing data on PFN for each series of isotopes. Since one does not know at present the percentage of scission neutrons in the total number of PFN, the comparison made here concerns only trends and not absolute values. A summary and conclusions can be found in Sec. VII.

II. EIGENVALUE PROBLEM

In the following section we will see that the main input in the calculation of the scission-neutron multiplicity ν_{sc} are the single-particle wave functions $|\Psi^i(\alpha_i)\rangle$ and $|\Psi^f(\alpha_f)\rangle$ that correspond to the eigenvalues $e^i(\alpha_i)$ and $e^f(\alpha_f)$ for the two nuclear configurations α_i and α_f , between which the sudden transition occurs.

Realistic wave functions are obtained by solving the eigenvalue problem:

$$\mathcal{H}\Psi = e\Psi, \quad (1)$$

with a Hamiltonian \mathcal{H} that includes the Laplacian, the nuclear potential, the spin-orbit coupling, and, for charged particles, the Coulomb potential [25]. The parameters are fitted to experimental single-particle and single-hole energies in the ^{208}Pb region [26]. An isospin dependence of the depth V_0 of the potential well [27] is assumed:

$$V_0 = V_{\text{mean}} \left[1 - C_{\text{iso}} \left(\frac{N - Z}{A} \right) \right] \quad (2)$$

with the constants $V_{\text{mean}} = 49.65$ MeV and $C_{\text{iso}} = 0.862$.

The main quantity in the Hamiltonian is the average potential in which the neutrons move. We choose it to be of Woods-Saxon type:

$$V(\rho, z) = -V_0 [1 + \exp(\Theta(\rho, z)/a_0)]^{-1} \quad (3)$$

where a_0 is the diffuseness.

We therefore need to estimate the distance Θ between each point in space (ρ, z) and the nuclear surface defined by the equation $\Phi(\rho, z, \alpha) = 0$. Axial symmetry is assumed. Close to scission, when the nuclear shape has a pronounced neck

(connecting the nascent fission fragments), this distance is no more uniquely defined. For this reason the procedure used to calculate Θ has been carefully checked to ensure that the results are correct and without discontinuities.

We have used two methods:

- (1) An exact numerical minimization of the distance between the given point (ρ, z) and any point on the nuclear surface.
- (2) An approximate formula based on a gradient approximation $\Theta(\rho, z) = \Phi(\rho, z)/|\nabla\Phi(\rho, z)|$ [21].

The numerical results for the distance for ^{236}U at a large deformation $\alpha = 0.900$ are presented in Fig. 1. The upper and lower panels correspond to the methods 1 and 2, respectively. One can see that the numerical minimization gives correct smooth curves while the gradient approximation overestimates the distance Θ in the neck region. Consequently the two methods yield to different behaviors of the diffuseness along the surface of an extremely deformed nucleus: constant or variable. A third potential minimum in the neck region is predicted by some time dependent Hartree-Fock calculations [28] so a variable diffuseness is not excluded. The effect of these two types of diffuseness on the SN multiplicities is studied in Sec. V.

Consequently we have included in the code “CASSINI” [23] (and in the related code “BARRIER” [24]) also a subroutine based on the exact evaluation by numerical minimization of the distance to the nuclear surface. The modified code has been tested at all deformations. We use this code to generate neutron wave functions in extremely deformed (i.e., just-before and immediately-after scission) fissioning nuclei and estimate scission-neutron multiplicities. The code BARRIER is used to consider nuclear pairing by a BCS method [24].

Due to the spin-orbit coupling the wave functions have two components, corresponding to spin “up” and spin “down” as follows:

$$|\Psi\rangle = f_1(\rho, z)e^{i\Lambda_1\phi}|\uparrow\rangle + f_2(\rho, z)e^{i\Lambda_2\phi}|\downarrow\rangle. \quad (4)$$

The values Λ_1 and Λ_2 are defined by

$$\Lambda_1 = \Omega - \frac{1}{2}, \quad \Lambda_2 = \Omega + \frac{1}{2}.$$

Ω is the projection of the total angular momentum along the symmetry axis, and it is the only good quantum number in the case of asymmetric fission. For symmetric fission the parity π is also conserved.

III. CHOICE OF THE TWO SCISSION CONFIGURATIONS

To describe the nuclear shapes just before and immediately after scission we use, as a zeroth-order approximation, Cassinian ovals [29] with only one deformation parameter: $\alpha_i = 0.985$ (i.e., $r_{\text{min}} = 0.179R_0$) and $\alpha_f = 1.001$ (i.e., $d_{\text{min}} = 0.047R_0$), respectively. d_{min} is the distance between the inner surfaces of the two fragments along the z axes. R_0 is the radius of the fissioning nucleus. In the case of ^{236}U these values are 1.5 and 0.8 fm, respectively. Note that $\alpha = 1.0$ describes a zero neck scission shape. It is known that these ovals are very close to the conditional equilibrium shapes, obtained by minimization of the deformation energy at a fixed value of the distance

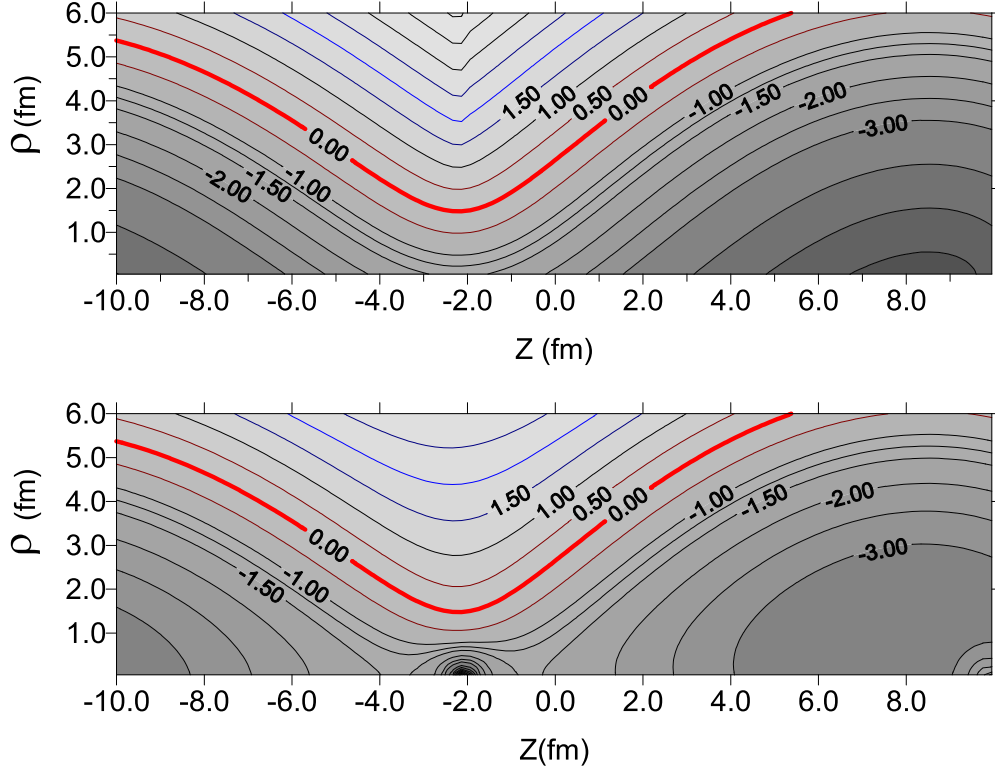


FIG. 1. Comparison between two methods used to calculate the distance from a given point (ρ, z) to the nuclear surface for a configuration with pronounced neck in ^{236}U .

between the centers of mass of the future fragments [30,31]. To include the asymmetric fission it is necessary to introduce a deviation from these ovals defined by a second parameter α_1 [21]. It turns out that r_{\min} and d_{\min} are almost independent of α_1 . The chosen value of the minimum neck radius is lower than predicted by dynamical calculations of the fission path with one-body dissipation [32] or by the optimal scission shapes [33] which is about 2 fm. If there are some indications on the value of r_{\min} , d_{\min} is, on the contrary, unknown.

Our choice (1.5 fm) goes back to the first calculation of SN multiplicity ν_{sc} in ^{236}U using the sudden approximation [3]. We found that using $r_{\min} = 1.9$ and $d_{\min} = 2.0$ fm leads to a too large value of ν_{sc} , equal to the total number of PFN detected in the reaction $^{235}\text{U}(n_{th}, f)$. This result was in contradiction with the general point of view (that we shared at that time) that SN represent a small fraction of PFN. We therefore took a lower value and kept it. This historical note shows that ν_{sc} is extremely sensitive to the choice of these two parameters that characterize the initial and final configurations involved in the diabatic process of neck rupture.

It is easy but not convincing to reproduce the total prompt neutron multiplicity $\langle \nu_p \rangle$ with an *ad hoc* set (r_{\min}, d_{\min}) before a more precise knowledge of these quantities is obtained from an adequate study. Moreover, if we accept the usual explanation of the existence of a minimum neck radius (at which the Coulomb repulsion can no more withstand the nuclear attraction), r_{\min} should slightly depend on (N_f, Z_f) . For the moment, the values used (0.179, 0.047 in units of R_0) are just working hypotheses. No attempt to tackle the problem of absolute ν_{sc} values is made here. Only relative behaviors are discussed.

IV. NEUTRON MULTIPLICITY: FORMALISM

The method of calculation is described in Ref. [3]. For completeness the relevant formulas are recapitulated below.

As mentioned in the Introduction the emission of scission neutrons is calculated in the sudden approximation of the scission process: the transition from two fragments connected by a thin neck ($\alpha_i = 0.985$) to two separated fragments ($\alpha_f = 1.001$) is supposed to happen infinitely fast. In this case the neutron wave functions of the α_i configuration experience a sudden change of the potential and become wave packets. The distribution of these neutron wave packets over the complete set of eigenstates of the α_f configuration,

$$|\Psi^i\rangle = \sum_f a_{if} |\Psi^f\rangle, \quad (5)$$

is essential in the calculation of the multiplicity of the neutrons released at scission;

$$a_{if} = \langle \Psi^i | \Psi^f \rangle = 2\pi \int (f_1^i f_1^f + f_2^i f_2^f) \rho d\rho dz. \quad (6)$$

$a_{if} \neq 0$ only if $|\Psi^i\rangle$ and $|\Psi^f\rangle$ have the same projection Ω of the total angular momentum along the symmetry axis.

The scission neutron multiplicity is given by the sum of the probabilities that a neutron occupying a given bound-state i is emitted, weighted by the occupation probability v_i^2 of the respective state i :

$$\nu_{sc} = 2 \sum_i v_i^2 \left(\sum_f |a_{if}|^2 \right). \quad (7)$$

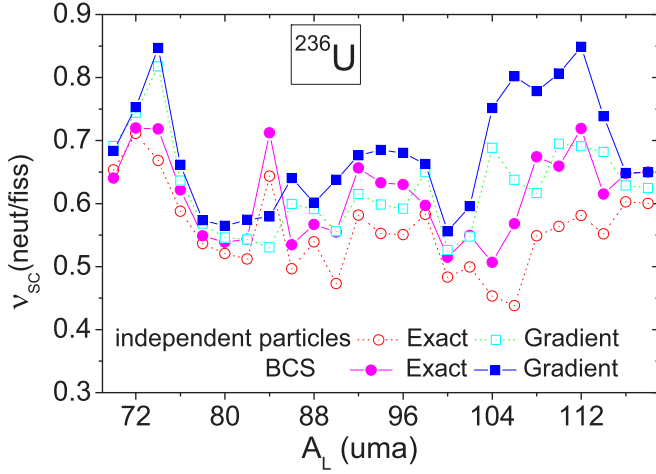


FIG. 2. Scission-neutron multiplicity as a function of mass asymmetry for two potentials (with the distance calculated exactly or using the gradient approximation) and for two occupation-probability functions (step or BCS). Although the mass asymmetry is defined by the mass of the light fragment, v_{sc} corresponds to the whole scissioning system.

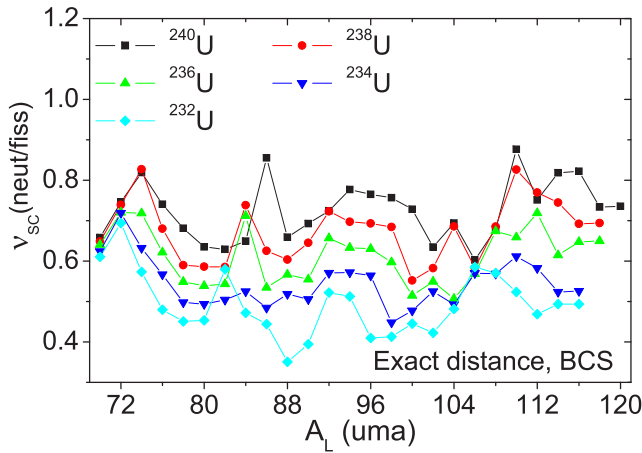
The i sum is over bound states while the f sum is over unbound states. In practice the sum over unbound states is replaced by 1 minus the sum over bound states. The factor 2 accounts for the fact that each of the two neutrons occupying a given state can be emitted.

Here we assume that the fissioning system is in its lowest energy state at α_i which means a superfluid descent from saddle to just-before scission. This is very probably the case in spontaneous and sub-barrier fission [34–37]. For independent neutrons v_i^2 is therefore a step function: it is 1 for states below the Fermi level and it is 0 above. If the neutrons are pairing correlated, v_i^2 is the BCS ground state occupation probability given by

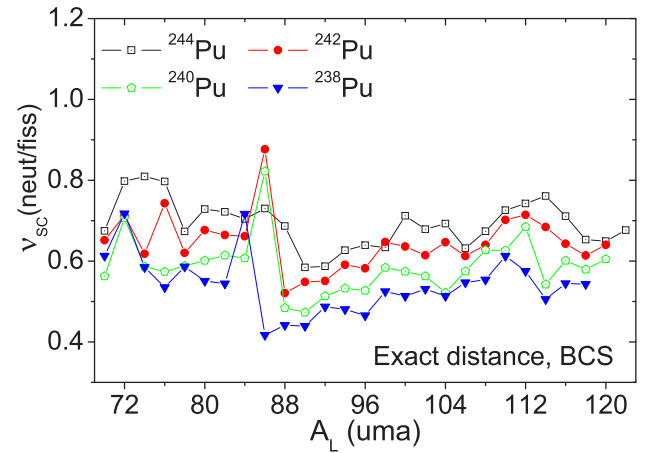
$$v_i^2 = \frac{1}{2} \left[1 - \frac{e_i - \lambda}{\sqrt{(e_i - \lambda)^2 + \Delta^2}} \right]. \quad (8)$$

If there is a nonzero temperature at α_i a similar smoothing of the step function takes place.

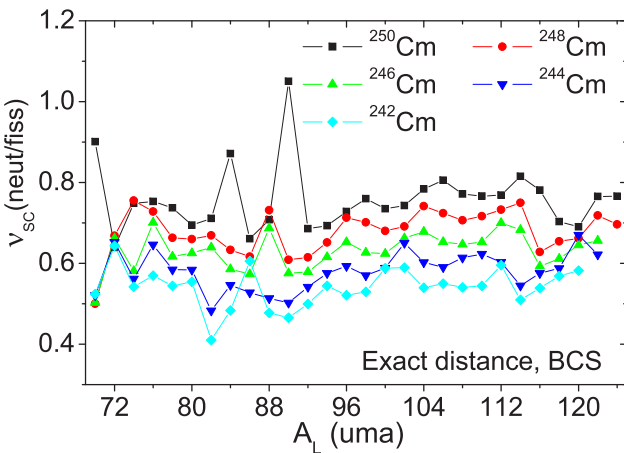
After the diagonalization of the Hamiltonian (see Sec. II), the neutron wave functions are obtained as an expansion in



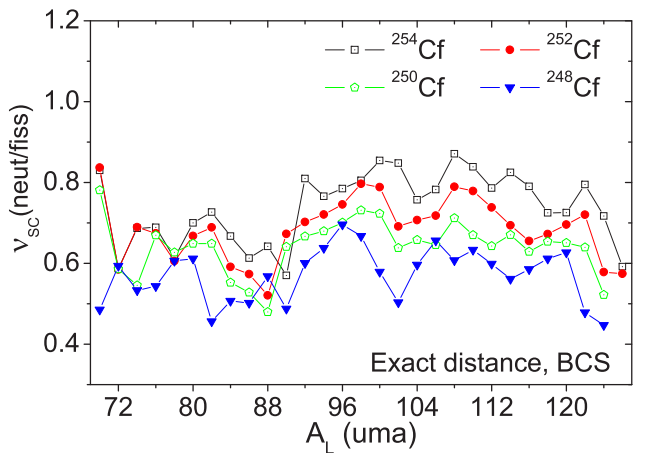
(a) U isotopes.



(b) Pu isotopes.



(c) Cm isotopes.



(d) Cf isotopes.

FIG. 3. Scission-neutron multiplicity as a function of mass asymmetry defined by the mass of the light fragment A_L . The distance is calculated exactly and BCS occupation probabilities are used.

the complete set of eigenstates of the deformed harmonic oscillators $|K_{\uparrow}\rangle$ and $|K_{\downarrow}\rangle$:

$$f_1^{i(f)} = \sum_k c_k^{i(f)}(1) |K_{\uparrow}\rangle,$$

$$f_2^{i(f)} = \sum_k c_k^{i(f)}(2) |K_{\downarrow}\rangle.$$

To avoid the numerical integration in Eq. (5) we choose the same basis of states for both diagonalizations (i.e., at α_f and at α_f). In this way the calculation of a_{if} is greatly simplified:

$$a_{if} = \sum_k c_k^i(1) c_k^f(1) + \sum_k c_k^i(2) c_k^f(2). \quad (9)$$

V. NEUTRON MULTIPLICITY: NUMERICAL RESULTS

We start by showing the effect of the different calculational hypotheses mentioned in Secs. II and IV on the scission-neutron multiplicities. The low-energy fission of ^{236}U [that simulates the reaction $^{235}\text{U}(n_{th}, f)$] is taken as an example.

We present in Fig. 2 the variation of the scission-neutron multiplicity ν_{sc} as a function of the light-fragment mass A_L obtained with two different Woods-Saxon potentials: one using the numerical minimization of the distance $\Theta(\rho, z)$ and the other using the gradient approximation (see Sec. II). For very deformed nuclei the two potentials are different as can be inferred from Fig. 1: in one the diffuseness is constant along the nuclear surface while in the other the diffuseness is smaller in the neck region. That is why the “exact” potential, which doesn’t exhibit a third well in the neck, produces less scission neutrons: there are less neutrons present in the neck region (where the diabatic coupling is most efficient [4]).

To show also the influence of the occupation probability $v_i^2(e_i)$ of the neutron states as a function of their energies (see Sec. IV), we added on Fig. 2 the results obtained with a step function (independent neutrons) and with Eq. (7) (pairing correlated neutrons). If we take pairing correlations into account we include in the sum over bound states in Eq. (6) states above the Fermi level that have higher emission probabilities [3] than the states below the Fermi level. For this reason the BCS curves are above the “independent particles” curves.

In the following figures we will present results obtained only with the BCS occupation probabilities and exactly estimated distances.

Figure 3(a) shows the dependence of the scission neutron multiplicity on the mass asymmetry of the fission fragments for even-even U isotopes from $A = 232$ to $A = 240$. The main trends that come out of this figure are

- the almost constant value of ν_{sc} for a given fissioning nucleus and
- the overall increase of ν_{sc} with the neutron number of the fissioning system N_f . This is because the number of neutrons available for emission is larger and not because the occupied states are less bound in neutron rich isotopes. In fact the values of the Fermi energy λ in these nuclei are not so different due to the isospin

dependence of V_0 (see Sec. II). The increase of R_0 with A is less than 1%, hence insignificant.

The observed small oscillations of ν_{sc} as a function of A_L are nuclear structure effects; at different mass asymmetries the sequence of states around the Fermi level is different. In ^{236}U the average value is 0.6 and the deviation from it is 0.06. Looking at different isotopes, these oscillations are in phase for two windows of mass asymmetry: around the most probable value and in the very asymmetric region.

Figures 3(b)– 3(d) show similar results but for Pu, Cm, and Cf isotopes, respectively. As before, for the same element Z , the neutron multiplicity increases with the neutron number N_f . There is no visible increase of ν_{sc} when we move from U ($Z_f = 92$) to Cf ($Z_f = 98$). If we look at the $N_f = 150$ isotones, one notices the opposite: a slight decrease from ^{244}Pu to ^{246}Cm and to ^{248}Cf .

VI. AVERAGE MULTIPLICITY: COMPARISON WITH EXISTING DATA

The average multiplicity $\langle \nu_{sc} \rangle$ can be obtained using $\nu_{sc}(A_L)$ from the previous section and the calculated primary-fragment fission mass yields $Y_{pre}(A_L)$ from the GEF model [38] or, when possible, from the experimental data themselves [39,40]:

$$\langle \nu_{sc} \rangle = \sum_{A_L} Y_{pre}(A_L) \nu_{sc}(A_L). \quad (10)$$

The latter choice is used in Fig. 4 where an example of input and output of Eq. (9) is plotted for the best experimentally studied systems: $^{235}\text{U}(n_{th}, f)$ and $^{252}\text{Cf}(sf)$. One notices that

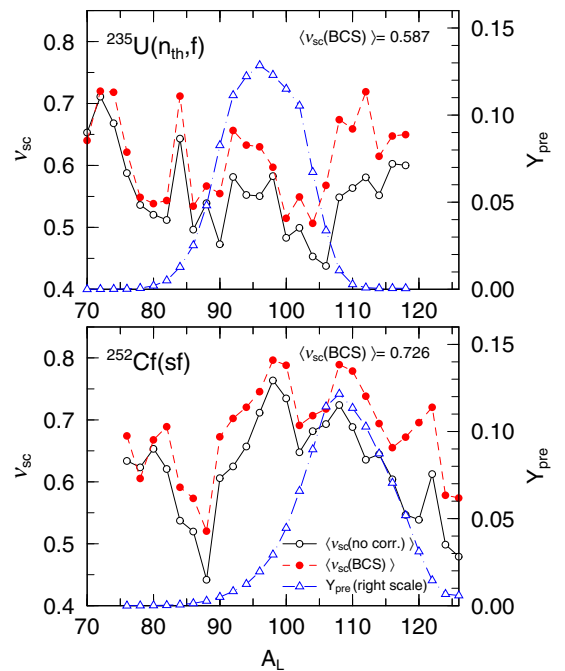


FIG. 4. Calculated scission-neutron multiplicity (left-hand scale) and experimental [39,40] preneutron mass yield (right-hand scale) as a function of light-fragment mass for $^{235}\text{U}(n_{th}, f)$ and $^{252}\text{Cf}(sf)$.

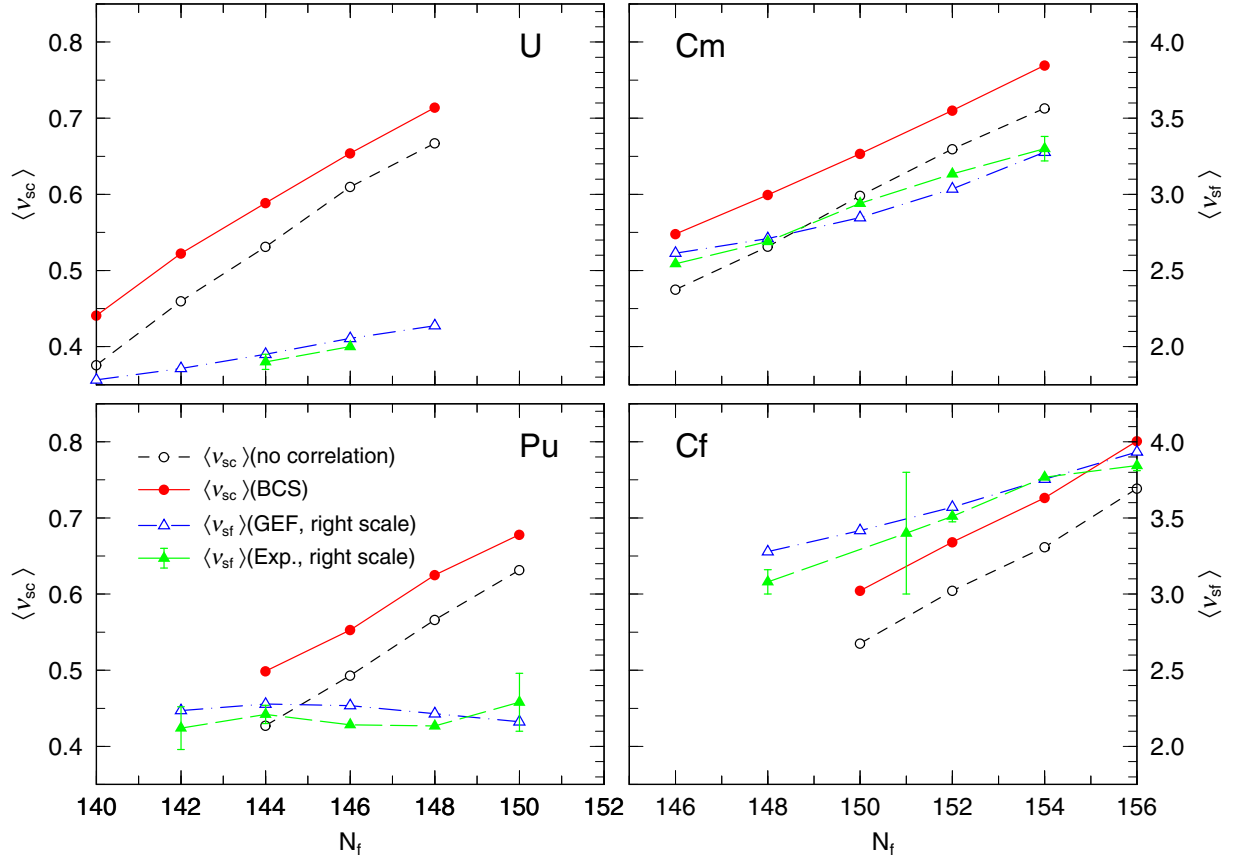


FIG. 5. Average SN multiplicity as a function of the neutron number N_f of the fissioning nucleus for U, Pu, Cm, and Cf isotopes. Calculated with the GEF model [38] and experimental [41] PFN multiplicities for spontaneous fission (or extrapolated to SF) are also plotted using a five-times larger right-hand scale to be able to directly compare the slopes.

the peak of Y_{pre} coincides better with a maximum of ν_{sc} in ^{252}Cf than in ^{236}U , and this is the second reason why calculated $\langle \nu_{sc} \rangle$ in $^{252}\text{Cf}(0.73)$ is 25% larger than the value calculated for ^{236}U (0.58). The first reason was the general increase of ν_{sc} with the neutron number N_f noticed in the previous section: ^{236}U has 144 neutrons while ^{252}Cf has 154. It is worth mentioning that the measured average PFN multiplicity (ν_p) is 55% larger in $^{252}\text{Cf}(sf)$ (3.76) than in $^{235}\text{U}(n_{th}, f)$ (2.43).

For the other fissioning nuclei we use fission yields calculated by GEF code. The resulting variation of $\langle \nu_{sc} \rangle$ as a function of the neutron number N_f is presented in Fig. 5 for the four series of isotopes studied. A clear increase is observed in all cases. It is mainly a consequence of the overall upwards shift of the ν_{sc} curves in Figs. 3(a)–3(d). Prompt neutron multiplicities $\langle \nu_{sf} \rangle$ for spontaneous fission calculated with GEF [38] and measured [41] are also included using a right-hand scale. The choice of the scales allows a direct comparison of the relative variation of $\langle \nu_{sc} \rangle$ and $\langle \nu_{sf} \rangle$ with N_f . One can see that in Cm and Cf isotopes the rate of increase is comparable with the calculated slope, in U isotopes it is less pronounced, and in Pu isotopes there is no increase at all. This exceptional experimental behavior of Pu isotopes is intriguing.

VII. SUMMARY AND CONCLUSIONS

The effect of a sudden nuclear-shape transition at scission on the emission of neutrons during low-energy fission is studied for four isotopic series corresponding to the elements U, Pu, Cm, and Cf. In each case the calculated variation of the SN multiplicity ν_{sc} with the mass ratio of the fission fragments A_L/A_H shows small oscillations around an almost constant average value that increases with the neutron number N_f of the respective isotope.

Due to the sudden approximation employed and to the neglected partial reabsorption of the unbound neutrons by the fragments, our approach gives only upper limits. With the present choice of scission configurations, SN represent at most 25% of the total number of PFN. It is however worth remembering that these estimates are very dependent on the minimum neck radius assumed just before scission and on the corresponding inner distance between the barely separated fragments. The value used here for r_{min} ($0.179R_0$) is less than our best knowledge of this quantity (2.0 fm) suggesting that this percentage may in reality be higher. However, as mentioned in the Introduction and at the end of Sec. III, only relative behaviors are discussed here. The problem of absolute values is left for a future study.

Finally, scission-neutron multiplicities averaged over all mass ratios, $\langle\nu_{sc}\rangle$, are calculated. An almost linear increase with the mass of the fissioning nucleus is found for all isotopes studied here. It reproduces the experimental trend in Cf and Cm, to a less extent in U, but not in Pu. An increase of $\langle\nu_{sc}\rangle$

from ^{236}U to ^{252}Cf is also obtained, which is similar to the PFN increase observed experimentally.

In conclusion, new properties of the scission neutrons are calculated and new similarities with the measured prompt fission neutrons are observed.

-
- [1] R. W. Fuller, *Phys. Rev.* **126**, 684 (1962).
- [2] I. Halpern, in *First Symposium on Physics and Chemistry of Fission* (IAEA, Vienna, 1965), Vol. II, p. 369.
- [3] N. Carjan, P. Talou, and O. Serot, *Nucl. Phys. A* **792**, 102 (2007).
- [4] N. Carjan and M. Rizea, *Phys. Rev. C* **82**, 014617 (2010).
- [5] N. Carjan, F.-J. Hamsch, M. Rizea, and O. Serot, *Phys. Rev. C* **85**, 044601 (2012).
- [6] M. Rizea and N. Carjan, *Nucl. Phys. A* **909**, 50 (2013).
- [7] M. Rizea and N. Carjan, *Proc. Rom. Acad. A*, **16**, 176 (2015).
- [8] N. Carjan and M. Rizea, *Phys. Lett. B* **747**, 178 (2015).
- [9] N. Feather, *Nature (London)* **143**, 597 (1939).
- [10] N. Feather, U. S. Atomic Energy Commission Document No. BR 335A, 1942 (unpublished); as quoted by Terrell in Ref. [11].
- [11] J. Terrell, *Phys. Rev.* **113**, 527 (1959).
- [12] D. G. Madland and J. R. Nix, *Nucl. Sci. Eng.* **81**, 213 (1982).
- [13] S. Lemaire, P. Talou, T. Kawano, M. B. Chadwick, and D. G. Madland, *Phys. Rev. C* **72**, 024601 (2005).
- [14] J. Randrup and R. Vogt, *Phys. Rev. C* **80**, 024601 (2009).
- [15] O. Litaize and O. Serot, *Phys. Rev. C* **82**, 054616 (2010).
- [16] R. Capote, Y.-J. Chen, F.-J. Hamsch, N. V. Kornilov, J. P. Lestone, O. Litaize, B. Morillon, D. Neudecker, S. Oberstedt, T. Ohsawa, N. Otuka, V. G. Pronyaev, A. Saxena, O. Serot, O. A. Shcherbakov, N.-C. Shu, D. L. Smith, P. Talou, A. Trkov, A. C. Tudora *et al.*, *Nucl. Data Sheets* **131**, 1 (2016).
- [17] C. B. Franklin, C. Hofmeyer, and D. W. Mingay, *Phys. Lett. B* **78**, 564 (1978).
- [18] H. R. Bowman, S. G. Thompson, J. C. D. Milton, and W. J. Swiatecki, *Phys. Rev.* **126**, 2120 (1962).
- [19] N. Kornilov, *Fission Neutrons (Experiments, Evaluation, Modeling and Open Problems)* (Springer International, Switzerland, 2015).
- [20] S. G. Nilsson, *Mat. Fys. Medd. Dan. Vid. Selsk.* **29**, 16 (1955).
- [21] V. Pashkevich, *Nucl. Phys. A* **169**, 275 (1971).
- [22] G. Ehrling and S. Wahlborn, *Phys. Scr.* **6**, 94 (1972).
- [23] E. Garrote, R. Capote, and R. Pedrosa, *Comput. Phys. Commun.* **92**, 267 (1995).
- [24] F. Garcia, O. Rodriguez, J. Mesa, J. D. T. Arruda-Neto, V. P. Likhachev, E. Garrote, R. Capote, and F. Guzmán, *Comput. Phys. Commun.* **120**, 57 (1999).
- [25] J. Damgaard, H. C. Pauli, V. V. Pashkevich, and V. M. Strutinsky, *Nucl. Phys. A* **135**, 432 (1969).
- [26] E. Rost, *Phys. Lett. B* **26**, 184 (1968).
- [27] P. E. Nemirowsky and V. A. Chepurinov, *Yad. Fiz.* **3**, 998 (1966).
- [28] D. Kolb, B. Y. Cusson, and H. W. Schmitt, *Phys. Rev. C* **10**, 1529 (1974).
- [29] V. S. Stavinsky, N. S. Rabotnov, and A. A. Seregin, *Yad. Fiz.* **7**, 1051 (1968).
- [30] V. M. Strutinsky, N. Ya. Lyashchenko, and N. A. Popov, *Nucl. Phys.* **46**, 639 (1963).
- [31] A. A. Seregin, *Yad. Fiz.* **55**, 2639 (1992).
- [32] A. J. Sierk, S. E. Koonin, and J. R. Nix, *Phys. Rev. C* **17**, 646 (1978).
- [33] F. A. Ivanyuk and K. Pomorski, *Phys. Rev. C* **79**, 054327 (2009).
- [34] H. Nifenecker, *Third Symposium on Physics and Chemistry of Fission, Rochester, NY, U.S.A., 1973* (IAEA, Vienna, 1974), Report No. IAEA STI/PUB/347, Vol. II, p. 435.
- [35] H. G. Borner, F. Gonnenswein, and O. Zimmer, *The Neutron: A Tool and an Object in Nuclear and Particle Physics* (World Scientific, Singapore, 2012), Chap. 4.7.3.
- [36] M. Rizea and N. Carjan, *Phys. Proc.* **31**, 78 (2012).
- [37] F. Ivanyuk and H. Hofmann, *Nucl. Phys. A* **657**, 19 (1999).
- [38] K.-H. Schmidt, B. Jurado, and Ch. Amouroux, NEA/DB/DOC 1, 2014.
- [39] A. Al-Adili, Ph.D. thesis, Uppsala University, Digital Comprehensive Summaries of Uppsala Dissertations from the Faculty of Science and Technology, No. 1002, 2013.
- [40] A. Gook, F.-J. Hamsch, and M. Vidali, *Phys. Rev. C* **90**, 064611 (2014).
- [41] H.-H. Knitter, U. Brosa, and C. Budtz-Jorgensen, in *The Nuclear Fission Process*, edited by C. Wagemans (CRC Press, Boca Raton, FL, 1991), Chap. 11, p. 514.